Incorporation of DOPE into Lipoplexes formed from a Ferrocene-Containing Lipid Leads to Inverse Hexagonal Nanostructures that allow Redox-Based Control of Transfection in High Serum

John P. E. Muller,[a] Burcu S. Aytar,[a] Yukishige Kondo,[b] David M. Lynn[a]* and Nicholas L. Abbott[a]*

[a]Department of Chemical and Biological Engineering, University of Wisconsin-Madison, 1415 Engineering Drive, Madison, Wisconsin 53706; [b]Department of Industrial Chemistry, Tokyo University of Science, Tokyo, Japan

Electronic Supplementary Information (ESI)

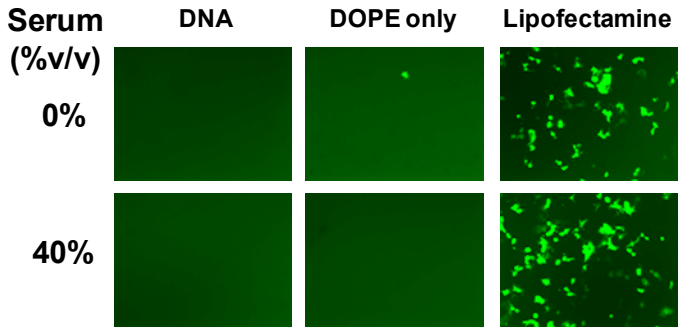

Fig. S1: Influence of serum on EGFP expression in COS-7 cells treated with pEGFP-N1 only (DNA) or with pEGFP-N1 and 10 μM DOPE (DOPE only, (φ_{DOPE} = 1)) or with commercial transfection agent (Lipofectamine 2000). The overall concentration of DNA in each solution was 2.4 μg/ml. Cells were incubated with the DNA or lipoplex solutions in Opti-MEM or 50% OptiMEM and 50% adult bovine serum for 4 h. Final concentration of Serum (BS) includes a 20% dilution effect from addition of DNA or lipoplex solution to each well. Images were acquired at 48 h after exposure of cells to lipoplexes. The dimensions of each micrograph above are 1194 μm by 895 μm.

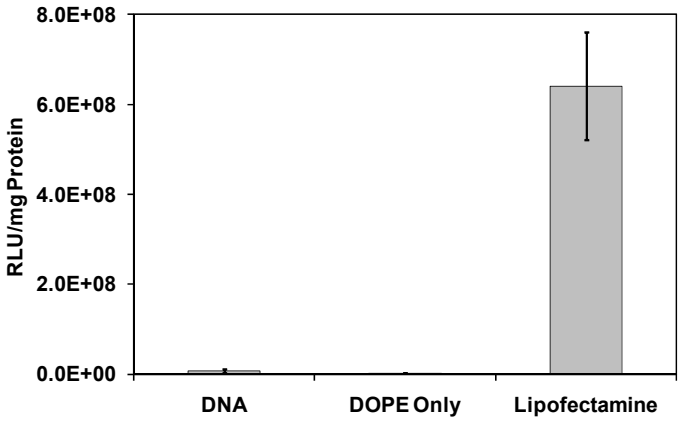

Fig. S2: Extent of normalized luciferase expression in COS-7 cells treated with pEGFP-N1 only (DNA) or with pEGFP-N1 and 10 μM DOPE (DOPE only, (φ_{DOPE} = 1)) or with commercial transfection agent (Lipofectamine 2000) for 4 h. All experiments were performed by adding 50 μL of DNA/lipid mixture in 1mM Li_2SO_4 solution to 200 μL of OptiMEM with cells present. DNA was present at a concentration of 2.4 μg/ml for all samples. Luciferase expression was measured 48 h after exposure to lipoplexes.

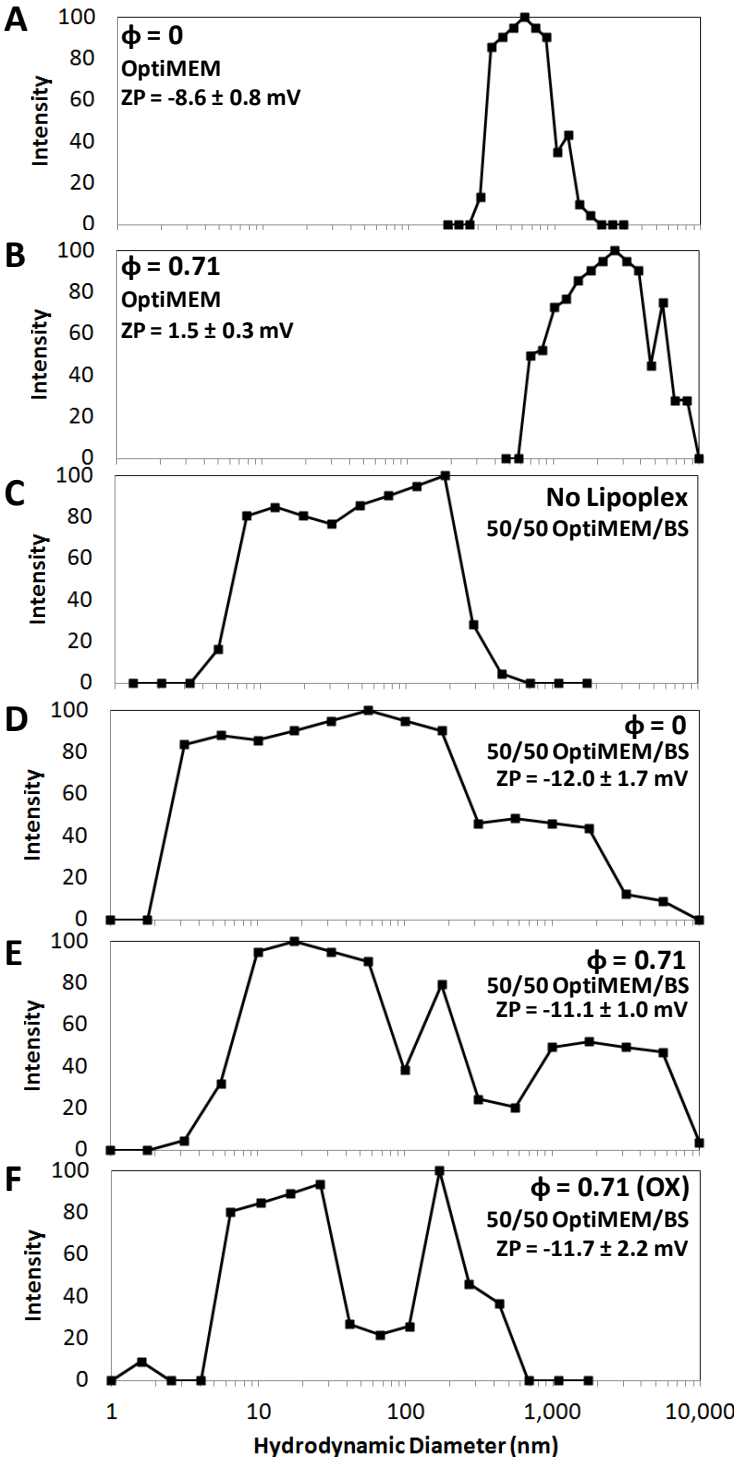

Fig. S3: Hydrodynamic diameters (plotted as an intensity-weighted distribution) and zeta potentials of **(A)** lipoplexes of $BFDMA_{RED}$ in OptiMEM, **(B)** lipoplexes of $BFDMA_{RED}$ and DOPE in OptiMEM, **(C)** OptiMEM containing 50% (v/v) BS in the absence of any lipoplexes, **(D)** lipoplexes of $BFDMA_{RED}$ in OptiMEM with 50% (v/v) BS, and **(E)** lipoplexes of $BFDMA_{RED}$ and DOPE in OptiMEM with 50% (v/v) BS **(F)** lipoplexes of $BFDMA_{OX}$ and DOPE in OptiMEM with 50% (v/v) BS; all lipoplexes were characterized after 20 minutes of incubation in the indicated media. Molar fractions of DOPE, φ_{DOPE} = DOPE/(BFDMA+DOPE), are given in the legend of each graph. DNA was present at a concentration of 2.4 μg/mL for all samples and the concentration of BFDMA in each sample was 8 μM. All experiments were repeated three times to confirm reproducibility of results.

Experiments designed to characterize the zeta potentials of lipoplexes, shown in Fig. S3 and Fig. S7, were conducted in the following general manner. Samples of lipoplexes formed from either $BFDMA_{RED}$ or $BFDMA_{RED}$-DOPE, or $BFDMA_{OX}$-DOPE were prepared as described above and in the main manuscript. These samples were then diluted using OptiMEM or OptiMEM with 50% (v/v) BS. For each sample, 5 mL of lipoplex solution was injected into the inlet of a Zetasizer 3000HS instrument, and measurements were made at ambient temperature using an electrical potential of 150 V. The final BFDMA and plasmid DNA (pEGFP-N1) concentrations were 8 μM and 24 mg/mL, respectively for all samples. These values are the same as those used in the cell transfection experiments described in the main manuscript. A minimum of five measurements was recorded for each sample, and the Henry equation was used to calculate zeta potentials from measurements of electrophoretic mobility. For this calculation, we assumed the viscosity of the solution to be the same as that of water.

Experiments designed to characterize the apparent size of lipoplexes, shown in Fig. S3, S4, S5 and S6, were conducted in the following general manner. A 100-mW, 532-nm laser (Compass 315M-100, Coherent, Santa Clara, CA) illuminated a temperature-controlled glass cell at 25 ^{o}C that was filled with a refractive-index matching fluid (decahydronaphthalene, Fisher Scientific, Pittsburgh, PA). The scattering of light was measured at an angle of 90^{o}. The autocorrelation functions (ACFs) were obtained using a BI-9000AT digital autocorrelator (Brookhaven Instruments, Holtsville, NY). The ACFs were analyzed using an intensity-based CONTIN analysis and then Stokes-Einstein relationship was used to yield hydrodynamic diameters as described previously (see Ref. 59 from the main manuscript). It is important to note that for lipoplexes with sizes greater than ~1 μm, the autocorrelation function can be influenced by rotational diffusion of the aggregates as well as internal degrees of freedom. For these reasons, the sizes of the larger complexes in Fig. S3, S4, S5 and S6 should be viewed as apparent hydrodynamic sizes.

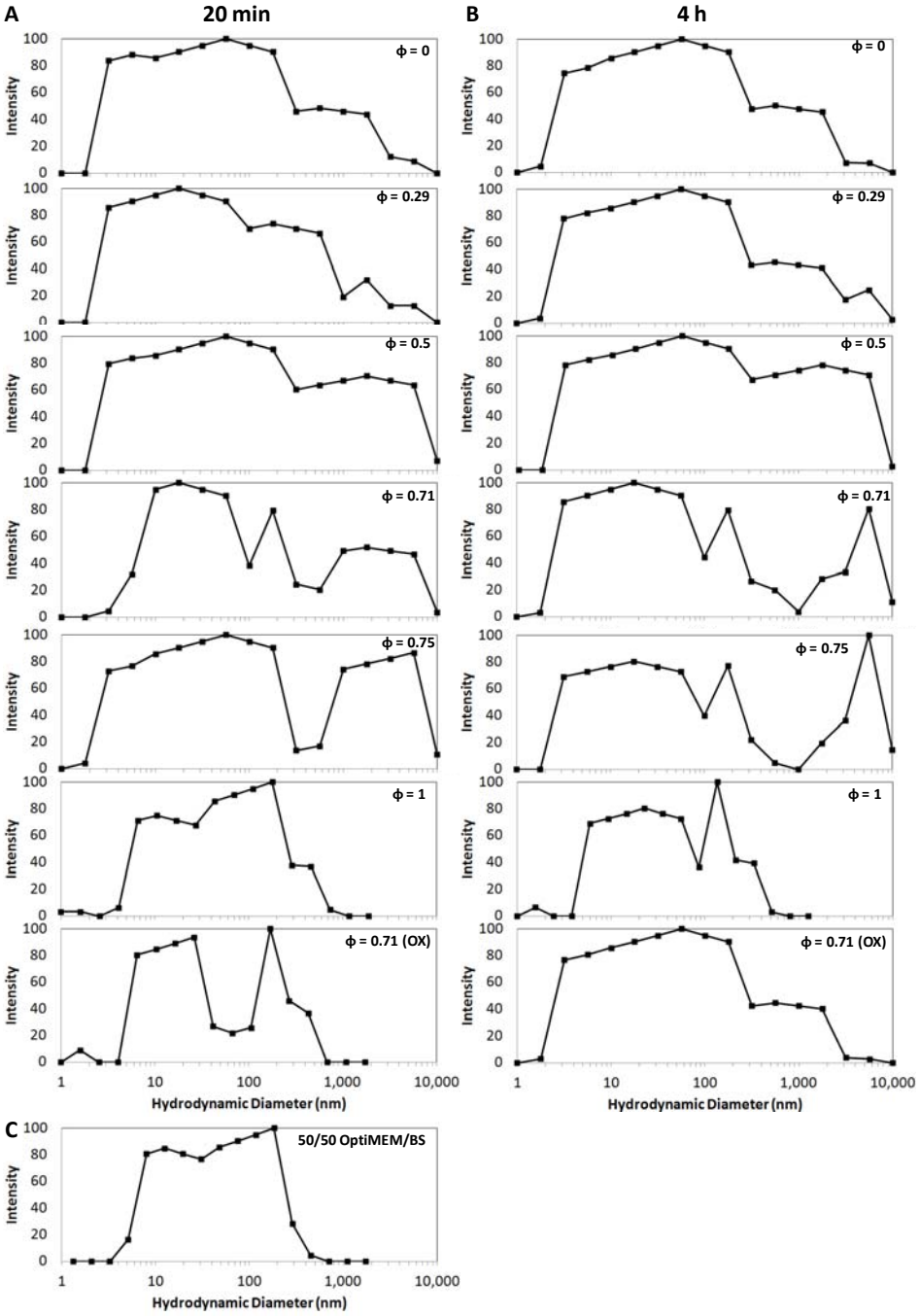

Fig. S4: Hydrodynamic diameters of lipoplexes (plotted as intensity-weighted distributions) formed using solutions of DNA and lipid ($BFDMA_{RED}$, $BFDMA_{OX}$ and/or DOPE), and incubated in OptiMEM with 50% (v/v) BS for **(A)** 20 minutes, **(B)** 4 hours. DNA was present at a concentration of 2.4 μg/mL for all samples. Mole fractions of DOPE, φ_{DOPE} = DOPE/(BFDMA+DOPE), are given in the legend of each graph. For $\varphi < 1$, $BFDMA_{RED}$ was used for all samples except where "(OX)" is indicated in the legend, denoting the presence of $BFDMA_{OX}$. The concentration of BFDMA in each sample was 8 μM. **(C)** Hydrodynamic diameters of aggregates found in OptiMEM with 50% (v/v) BS.

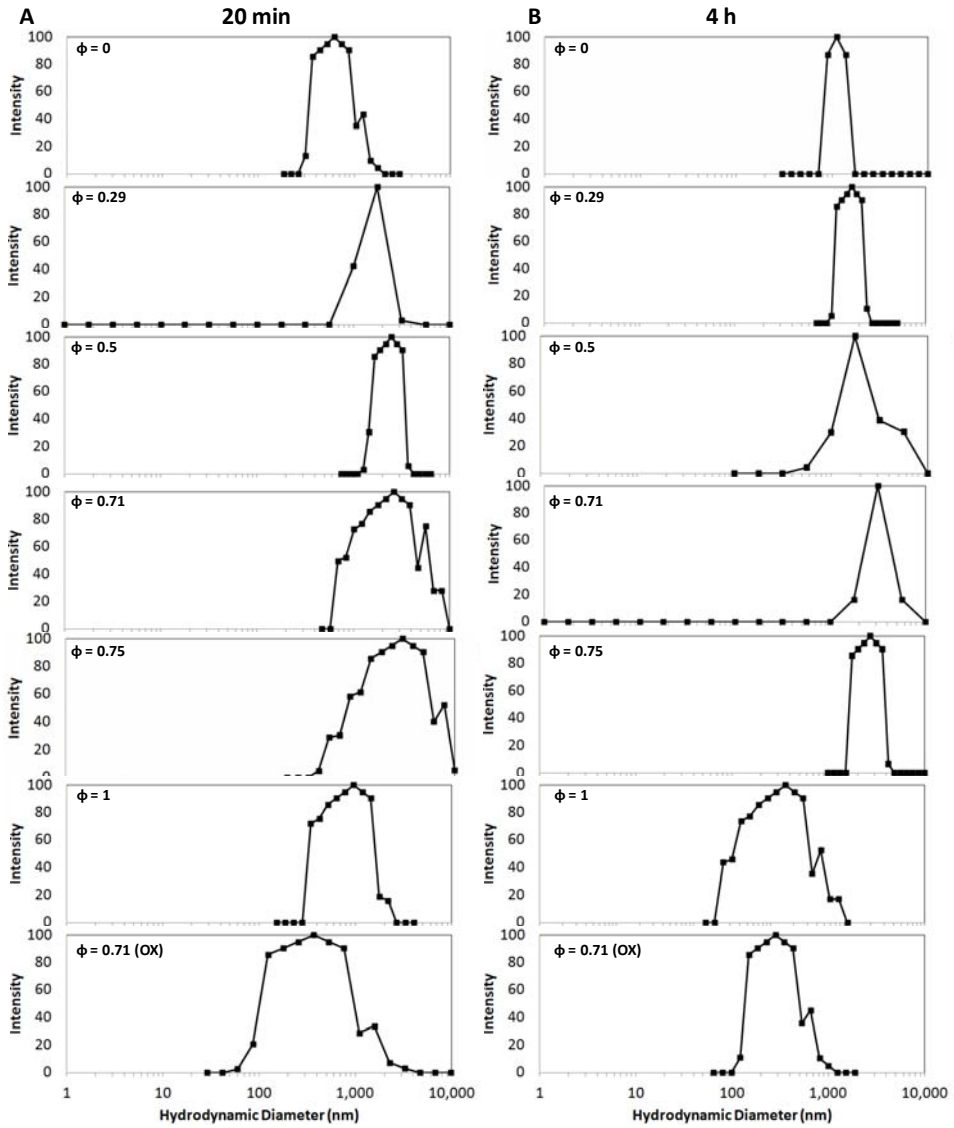

Fig. S5: Hydrodynamic diameters of lipoplexes (plotted as intensity-weighted distributions) formed using solutions of DNA and lipid ($BFDMA_{RED}$, $BFDMA_{OX}$ and/or DOPE), and incubated in OptiMEM for **(A)** 20 minutes, **(B)** 4 hours. DNA was present at a concentration of 2.4 μg/mL for all samples. Mole fractions of DOPE, φ_{DOPE} = DOPE/(BFDMA+DOPE), are given in the legend of each graph. For $\varphi < 1$, $BFDMA_{RED}$ was used for all samples except where "(OX)" is indicated in the legend, denoting the presence of $BFDMA_{OX}$. The concentration of BFDMA in each sample was 8 μM.

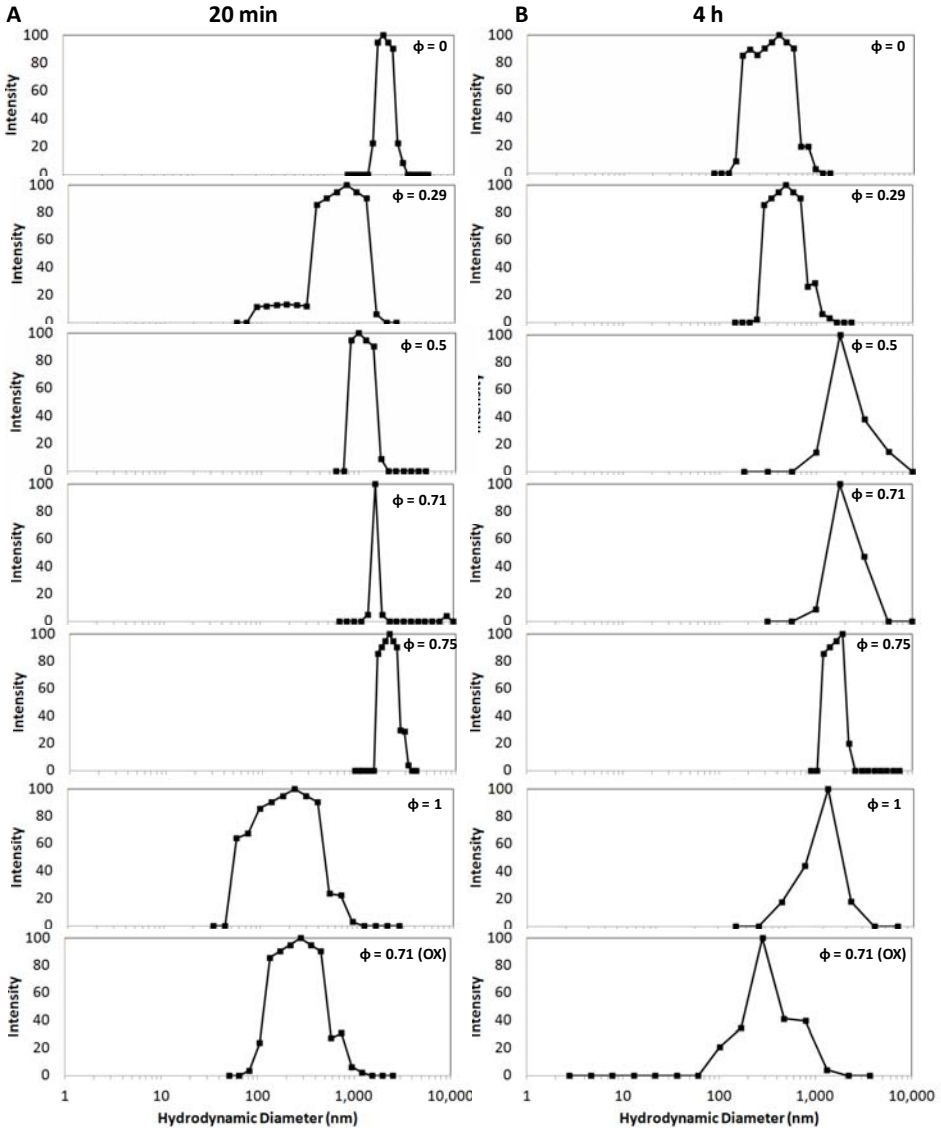

Fig. S6: Hydrodynamic diameters of lipoplexes (plotted as intensity-weighted distributions) formed using solutions of DNA and lipid ($BFDMA_{RED}$, $BFDMA_{OX}$ and/or DOPE), and incubated in 1 mM Li_2SO_4 for **(A)** 20 minutes, **(B)** 4 hours. DNA was present at a concentration of 2.4 μg/mL for all samples. Mole fractions of DOPE, φ_{DOPE} = DOPE/(BFDMA+DOPE), are given in the legend of each graph. For $\varphi < 1$, $BFDMA_{RED}$ was used for all samples except where "(OX)" is also indicated in the legend, denoting the presence of $BFDMA_{OX}$. The concentration of BFDMA in each sample was 8 μM.

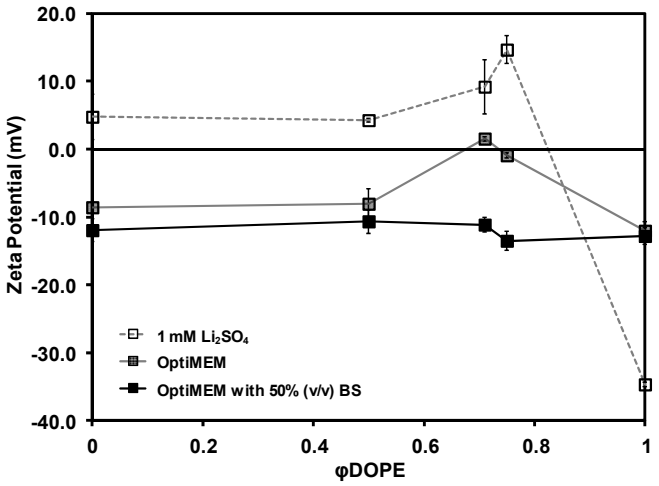

Fig. S7: Zeta potentials of lipoplexes of BFDMA and/or DOPE and DNA, plotted as a function of mole fraction of DOPE (φ_{DOPE}). BFDMA is present at 8 μM and DNA at 2.4 μg/mL resulting in a charge ratio of 1.1 for all samples with $\varphi < 1$. The symbols correspond to different media, specified in the legend. Error bars represent the standard deviation of five measurements. Note that the zeta potential, when measured in OptiMEM containing 50% (v/v) BS, remains constant, around -11 ± 1 mV, for $\varphi_{DOPE} = 0$ to 1.

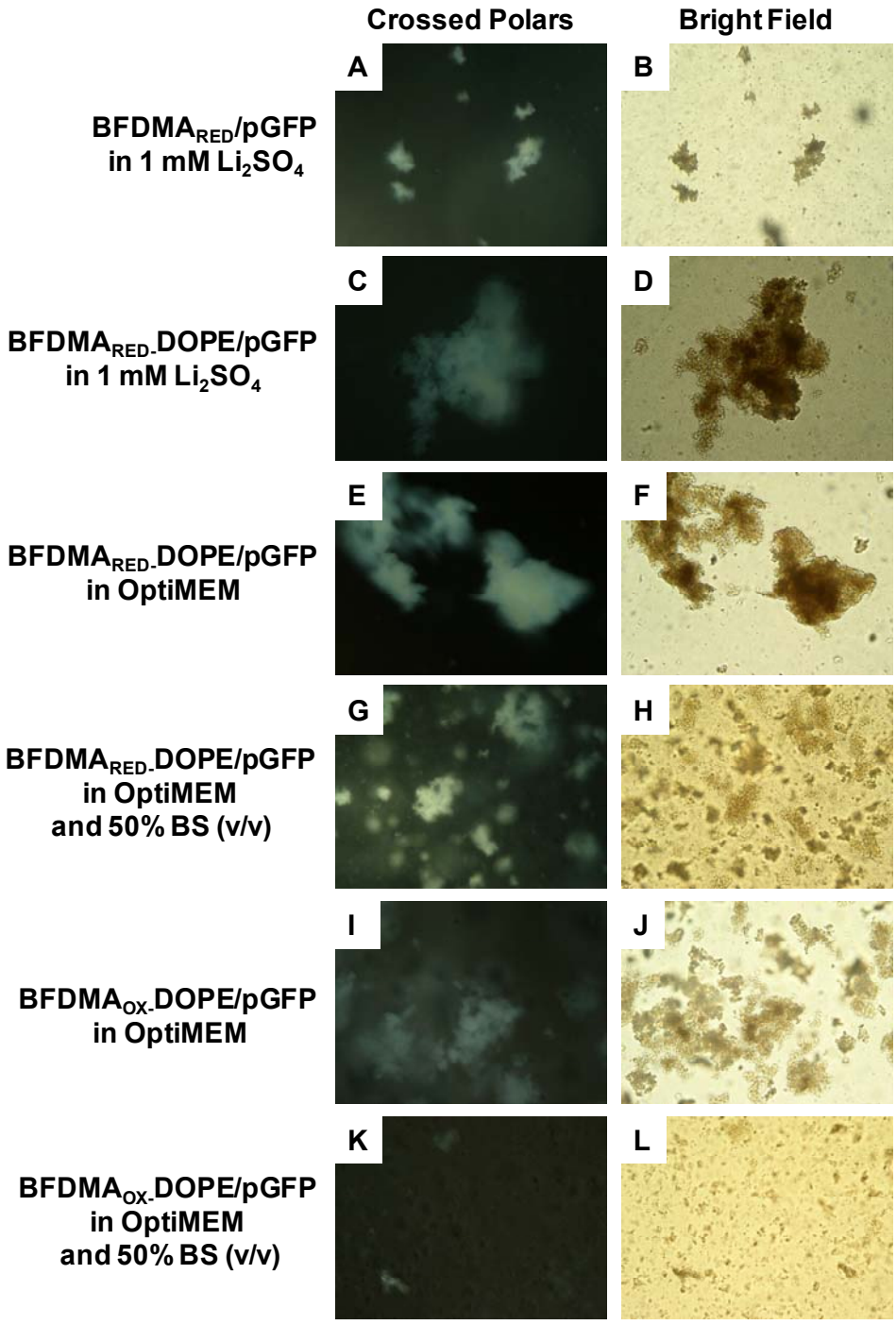

Fig. S8: Optical images (crossed polars, left column and bright field, right column) of lipoplexes of either BFDMA alone ($\varphi_{DOPE} = 0$) or BFDMA-DOPE ($\varphi_{DOPE} = 0.71$) and pGFP DNA used to determine the presence of birefringence. The lipid concentrations in each sample are, **(A and B)** 0.87 mM BFDMA; **(C and D)** 0.87 mM BFDMA and 2.17 mM DOPE; **(E, F, I and J)** 0.64 mM BFDMA and 1.60 mM DOPE; **(G, H, K and L)** 0.32 mM BFDMA and 0.8 mM DOPE; all in the presence of pEGFP-N1 (2.0 mg/ml) at a charge ratio of 1.1:1 or 3.3:1 (+/-) for reduced or oxidized BFDMA containing solutions respectively. Media used for each sample is indicated on the left side of each figure. Width of each micrograph corresponds to 880 μm. Note that the concentrations of BFDMA in these samples are approximately 1000-fold higher than those used in transfection experiments, and thus the sizes of the aggregates in these images should not be used to indicate the sizes of lipoplexes that lead to cell transfection.

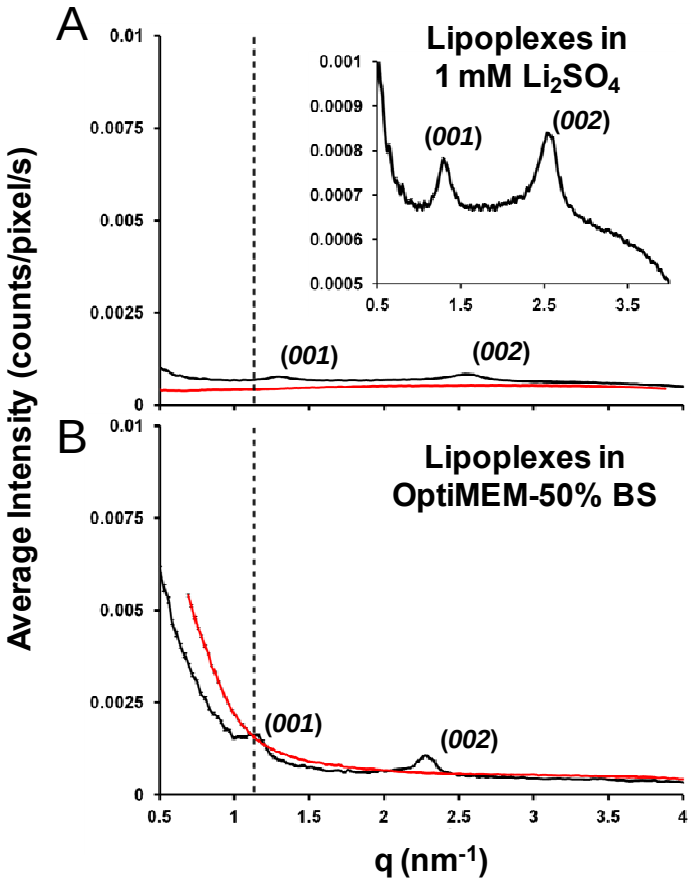

Fig. S9: SAXS spectra obtained using reduced BFDMA (black) or oxidized BFDMA (red) containing solutions of; **(A)** 0.87 mM BFDMA in 1 mM Li_2SO_4; **(B)** 0.32 mM BFDMA in OptiMEM with 50% (v/v) BS, all in the presence of pEGFP-N1 (2.0 mg/ml) at a charge ratio of 1.1:1 or 3.3:1 (+/-) for reduced or oxidized BFDMA containing solutions respectively.

Comments regarding cubic nanostructures: Cubic phases reported in the literature include, (i) the space group *Ia3d* (Q^{230}) with experimentally visible Bragg peaks at √6, √8, √14, √16, and √20. This is the most commonly observed bicontinuous cubic phases in surfactant and lipid systems.[1-6] Here we also note that ref. 2 by Lindblom et al. specify the *Ia3d* space group as √3, √4, √7, √8, etc. However, in *International Tables* (p. 345-346)[7] no odd integer roots are allowed in the spacings, in disagreement with ref 92. (ii) the space group *Pn3m* (Q^{224}), a primitive cubic lattice with the spacing √2, √3, √4, √6, √8, √9, √10 etc., shown to exist, for example, in solutions containing DOPE-Me,[8] (iii) the space group *Im3m* (Q^{229}), a body-centred cubic lattice with the spacing √2, √4, √6, √8, √10 √12, √14 etc., a less common structure that has been observed in several lipid systems.[2, 8]

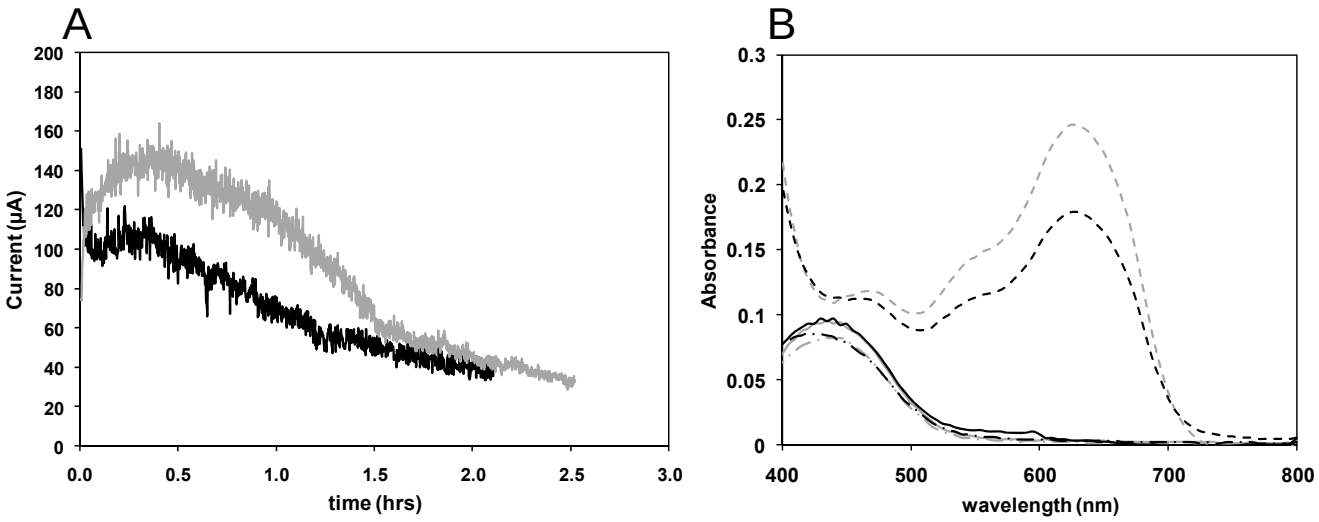

Fig. S10: (A) Current passed over time at a potential of 600 mV during the electrochemical oxidation of 1 mM BFDMA, $\varphi_{DOPE} = 0$ (light solid line) and 1 mM BFDMA in the presence of 2.5 mM DOPE, $\varphi_{DOPE} = 0.71$ (dark solid line), in 1 mM Li_2SO_4; **(B)** UV/visible absorbance spectra for solutions of BFDMA only ($\varphi_{DOPE} = 0$); reduced BFDMA (light line), electrochemically oxidized BFDMA (light dashed line), oxidized BFDMA treated with a 10 fold excess of ascorbic acid to chemically reduce an electrochemically oxidized sample (light dot-dashed line). The solutions were aqueous in 1 mM Li_2SO_4 containing 500 μM reduced or oxidized BFDMA respectively. UV/visible absorbance spectra for solutions of BFDMA and DOPE ($\varphi_{DOPE} = 0.71$); reduced BFDMA/DOPE (dark line), electrochemically oxidized BFDMA/DOPE (dark dashed line), oxidized BFDMA/DOPE treated with a 10 fold excess of ascorbic acid (dark dot-dashed line). The solutions were aqueous in 1 mM Li_2SO_4 containing 500 μM reduced or oxidized BFDMA in the presence of 1.25 mM DOPE. For all samples, prior to absorbance measurements, DTAB was added to eliminate turbidity observed in the lipid solutions. DOPE, ascorbic acid and DTAB do not absorb light in the region of 400-800 nm.

To electrochemically oxidize BFDMA in the presence of DOPE for use in cell transfection experiments, we used a solution of 1 mM BFDMA and 2.5 mM DOPE in aqueous 1 mM Li_2SO_4 ($\varphi_{DOPE} = 0.71$), a composition chosen on the basis of the results shown in Figures 2 and 3. A platinum gauze electrode was immersed into the solution and held at a potential of 600 mV (vs. Ag/AgCl standard electrode) for 3 h at 75 ^oC. This elevated temperature was used because in past studies it has been found that the rate of oxidation of BFDMA alone is significantly enhanced at this temperature. Spectrophotometry was used to characterize the extent of oxidation of BFDMA in the resulting solution and the results were compared to previous studies (see Figure S10 above). In brief, spectrophotometric measurements confirmed that the presence of DOPE during electrochemical oxidation did not prevent the oxidation of $BFDMA_{RED}$ to $BFDMA_{OX}$ (see structure shown in Figure 1A). The absorbance spectrum of $BFDMA_{RED}$ was similar to $BFDMA_{RED}$-DOPE and, upon electrochemical oxidation, the absorbance spectrum of $BFDMA_{OX}$ was similar to $BFDMA_{OX}$-DOPE (Figure S10). We also note that subjecting a solution of 2.5 mM DOPE to a potential of 600 mV led to no significant passage of current over a period of 3 h. We conclude on the basis of these results that the procedure described above can be used to electrochemically oxidize BFDMA in the presence of DOPE.

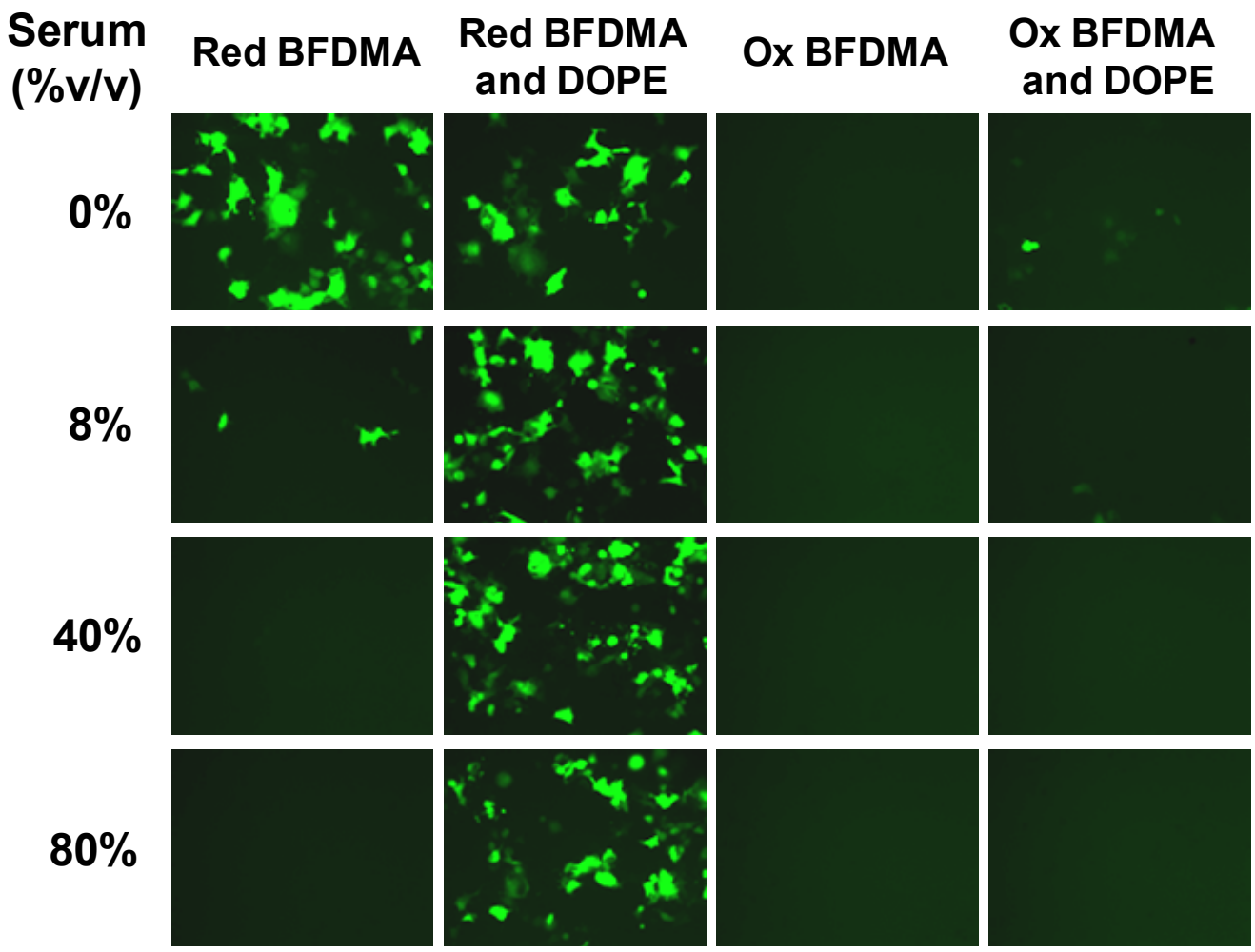

Fig. S11: Influence of serum on EGFP expression in COS-7 cells treated with lipoplexes formed from pEGFP-N1 and reduced or oxidized BFDMA with ($\varphi_{DOPE} = 0.71$) and without ($\varphi_{DOPE} = 0$) DOPE for 4 h. Cells were incubated with the lipoplex solutions in Opti-MEM and different levels of BS (given down the left hand side of the figure). The overall concentrations of BFDMA and DNA in each lipoplex solution were 8 μM and 2.4 μg/ml, respectively, providing a charge ratio of 1.1:1 (+/-) for all reduced BFDMA samples and 3.3 for oxidized BFDMA samples as DOPE has a net charge of zero. Fluorescence micrographs (1194 μm by 895 μm) were acquired 48 h after exposure of cells to lipoplexes. No evidence of cell transfection was seen for DOPE only containing lipoplexes (see Figures S1 and S2 in Supporting Information).

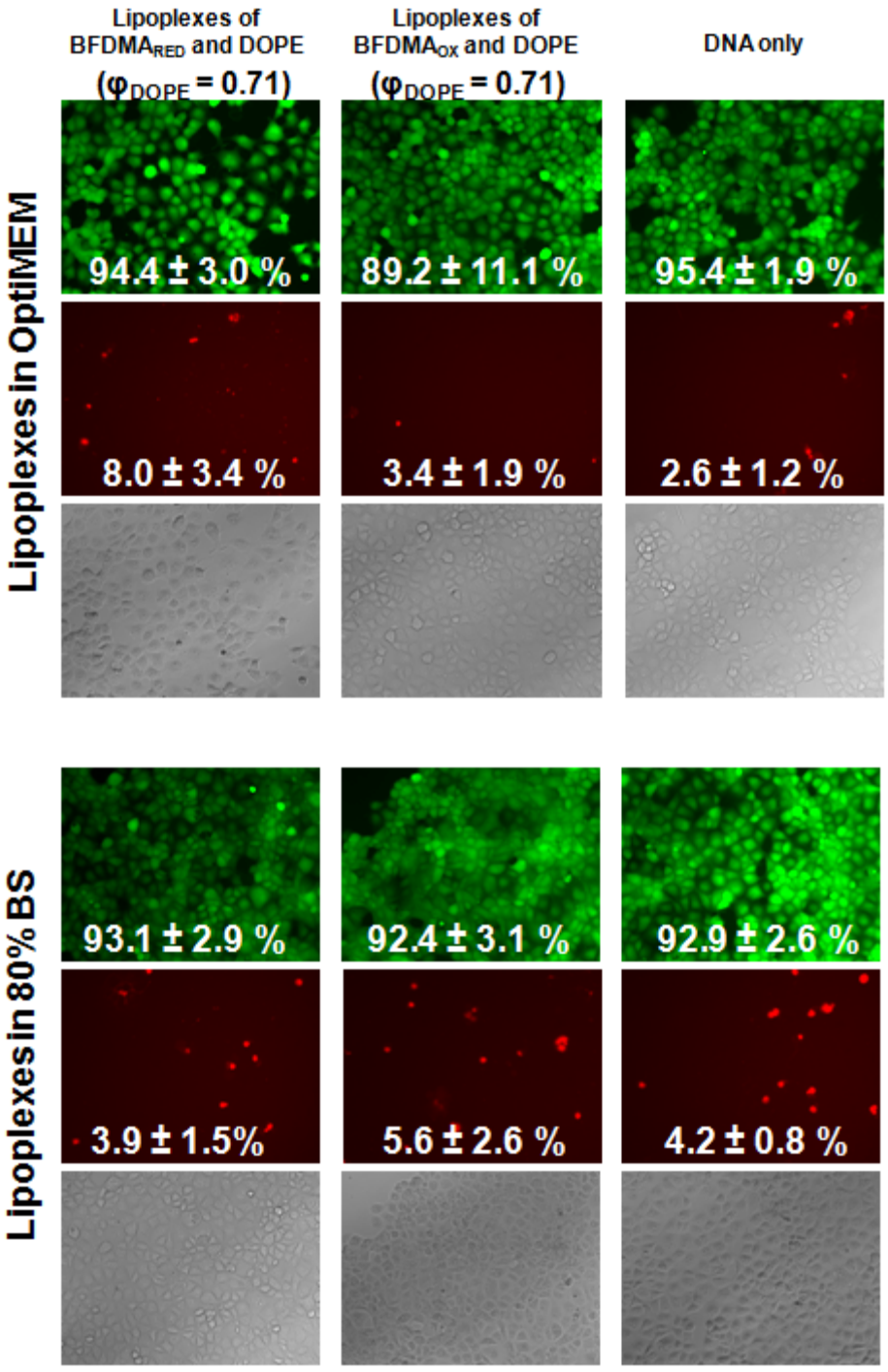

Fig. S12: Results of live/dead cytotoxicity assays for COS-7 treated with lipoplexes formed from BFDMA$_{RED}$-DOPE, BFDMA$_{OX}$-DOPE, and DNA only (as a negative control). Plasmid DNA encoding luciferase was used to form the lipoplexes used in these experiments. Cells were exposed to lipoplexes for 4 h in OptiMEM (Top), or 80% BS (Bottom). Representative fluorescence and phase-contrast micrographs were captured 48 h after exposure to lipoplexes or DNA. Cells were stained with each of the following respective live/dead cell stains and allowed to sit for 30 minutes prior to imaging: Calcein AM was used to reveal live cells and appears as green fluorescence; EthD-1 was used to reveal dead cells and is shown as red fluorescence. Values for the percentage of live cells in each image were calculated using the number of Calcein AM-stained cells and the total number of cells determined by Hoechst (nuclear) stained cells (data not shown). The percentage of dead cells was calculated using the number of EthD-1-stained cells and the total number of Hoechst stained cells. These percentage values are shown in the figure above on each of the respective fluorescent micrographs. The error shown in the data is one standard deviation, n = 5.

Table S1: Results of live/dead cytotoxicity assays for COS-7 treated with lipoplexes formed from $BFDMA_{RED}$, $BFDMA_{RED}$-DOPE, $BFDMA_{OX}$-DOPE, and DNA only (as a negative control). Experiments were performed in OptiMEM media, or in OptiMEM containing increasing concentration of BS (8%, 40%, or 80% (v/v)). In each entry in the Table, "L" refers to the percentage of live cells, and "D" refers to the percentage of dead cells. For details of lipoplex preparation and methods used to determine the percentage of live and dead cells, see the caption to Figure S10.

	% Live cells (L) and % Dead cells (D)			
	OptiMEM	**8% BS**	**40% BS**	**80% BS**
$BFDMA_{RED}$ + DNA	L: 90.8 ± 1.7 D: 6.2 ± 1.0	-	-	-
$BFDMA_{RED}$-DOPE + DNA	L: 94.4 ± 3.0 D: 8.0 ± 3.4	L: 89.4 ± 8.0 D: 5.5 ± 4.4	L: 96.1 ± 2.8 D: 3.5 ± 2.5	L: 93.1 ± 2.9 D: 3.9 ± 1.5
$BFDMA_{OX}$-DOPE + DNA	L: 89.2 ± 11.1 D: 3.4 ± 1.9	L: 89.9 ± 4.4 D: 5.0 ± 2.3	L: 96.2 ±3.4 D: 3.6 ± 1.4	L: 92.4 ± 3.1 D: 5.6 ± 2.6
DNA only	L: 95.4 ± 1.9 D: 2.6 ± 1.2	L: 90.1 ± 3.8 D: 3.1 ± 0.8	L: 88.2 ± 3.3 D: 5.0 ± 1.9	L: 92.9 ± 2.6 D: 4.2 ± 0.8

Electronic Supplementary Information References

1. P. Alexandridis, U. Olsson and B. Lindman, *Langmuir*, 1998, **14**, 2627-2638.
2. G. Lindblom and L. Rilfors, *Biochimica Et Biophysica Acta*, 1989, **988**, 221-256.
3. K. Fontell, *Colloid Polym. Sci.*, 1990, **268**, 264-285.
4. R. Ivanova, B. Lindman and P. Alexandridis, *Langmuir*, 2000, **16**, 3660-3675.
5. R. Ivanova, B. Lindman and P. Alexandridis, *Langmuir*, 2000, **16**, 9058-9069.
6. V. Luzzati and P. A. Spegt, *Nature*, 1967, **215**, 701-704.
7. *International Tables for X-Ray Crystallography, 1*, 2nd edn., The Kynoch Press, Birmingham, 1965.
8. S. M. Gruner, M. W. Tate, G. L. Kirk, P. T. C. So, D. C. Turner, D. T. Keane, C. P. S. Tilcock and P. R. Cullis, *Biochemistry*, 1988, **27**, 2853-2866.